A Terahertz Band-Pass Filter Based on Coplanar-Waveguide and Spoof Surface Plasmon Polaritons

Shizhuang Yan, *Student Member, IEEE*, Jun Wang, *Member, IEEE*, Xianglin Kong, *Student Member, IEEE*, Ruofeng Xu, Zhao-Min Chen, Jian-Yu Ma, and Lei Zhao, *Senior Member, IEEE*

***Abstract*— A THz ultra-broadband band-pass filter based on coplanar-waveguide and spoof surface plasmon polaritons (SSPPs) is proposed, which can be operated from 0.65 THz to 2.02 THz with high efficiency and compact size. Additionally, the lower and upper cut-off frequencies of the proposed filter can be controlled independently by changing the corresponding parameters. The interdigital structure is used to filter the low frequency wave, meanwhile, the SSPPs is designed for producing the upper cut-off frequency. The operating principles are explained by dispersion curves and field distributions. The return loss and insertion loss of the proposed filter are higher than 11 dB and less than 2 dB in the passband, respectively. For validating the proposed band-pass filter design concept, a prototype of a filter operating at millimeter-wave frequency is fabricated and measured, and the measured results have a good agreement with the simulated ones.**

***Index Terms*— Band-pass filter, coplanar waveguide, spoof surface plasmon polaritons, terahertz filter.**

I. Introduction

WITH the rapid development of terahertz technology, it is important and urgent to design and manufacture terahertz devices. Terahertz filter is an indispensable operating device in sensor, communication system and imaging application. In recent years, various technologies have been reported for the development of THz filters [1]–[8]. In [6], a 140-GHz LTCC substrate integrated waveguide (SIW) filter based on electric coupling was introduced, whose minimum insertion loss of the filter is up to 1.913 dB. Moreover, a 140-GHz LTCC SIW filter based on magnetic coupling structure was proposed to improve the insertion loss [7]. However, the bandwidth of the two filters should be expanded for future communication system. Accordingly, a terahertz filter using double-stacked metamaterial layers separated by an air gap was proposed, which realized a wide bandwidth from 0.2 THz to 0.8 THz [2]. Nevertheless, the transmission efficiency needs to be further improved. In [8], a terahertz dual-resonance band-pass filter using bilayer reformative complementary metamaterial structures was presented, which realized objective of improving the filtering performance. Nevertheless, compared with other types of filters, this kind of structure is slightly complex. Therefore, seeking an efficient method to realize low insertion loss, miniaturized, wide bandwidth and planar THz band-pass filter is technically challenging.

Nowadays, with the development of spoof surface plasmon polaritons (SSPPs) technology, making it possible to design THz filters with simple structure, controllable frequency and excellent transmission characteristics. Recently, a variety of filters based on SSPP technology have been proposed in [9]–[24]. In [12], Nagendra *et.al* presented a SSPP-based reconfigurable band-pass filter, whose cut-off frequency can be controlled by SSPP T-shape resonator and variable capacitor device. However, the performance in frequency-controlling of the filter needs to be enhanced. In order to solve this problem, another SSPP band-pass filter with higher frequency selectivity and wide rejection bandwidth is proposed [13], which achieves a bandwidth from 0.17-0.52 THz with 87.85% relative bandwidth. Nevertheless, the insertion loss needs to be improved. Accordingly, a THz SSPP filter based on compact balanced coplanar stripline was designed, whose cut-off frequency can be easily controlled [15]. Moreover, a terahertz filter based on SSPP waveguide and Archimedean spirals was designed in [21], which has the distinguishing feature of frequency selectivity and low insertion loss.

In this letter, we proposed a THz band-pass filter based on CPW and SSPPs with the interdigital structure etch on its middle metal line. The proposed THz band-pass filter has a return loss of more than 11 dB and an average insertion loss of 2 dB in the passband from 0.65 THz to 2.02 THz. A prototype of the band-pass filter operating at millimeter-wave frequency is fabricated and measured. The measured and simulated results show a good agreement, indicating that the proposed design has potential applications for engineering.

II. Theory and Method

A. The Proposed SSPP Unit Cell and Dispersion Curves

Fig. 1(a) illustrates the top view of the unit cell of proposed THz SSPP, which is periodically made into a metal film on

Manuscript received February 6, 2022; revised March 12, 2022; accepted March 13, 2022. Date of publication March 16, 2022; date of current version March 24, 2022. This work was supported in part by the National Natural Science Foundation of China under Grant 61771226. *(Corresponding author: Lei Zhao.)*

Shizhuang Yan, Jun Wang, Xianglin Kong, Ruofeng Xu, and Lei Zhao are with the School of Information and Control Engineering, China University of Mining and Technology, Xuzhou 221116, China (e-mail: szyanmax@163.com; jun-wang@cumt.edu.com; xlkong@cumt.edu.cn; xuruofeng@cumt.edu.cn; leizhao@cumt.edu.cn).

Zhao-Min Chen and Jian-Yu Ma are with the State Key Laboratory of Millimeter Waves, School of Information Science and Engineering, Southeast University, Nanjing 210096, China (e-mail: drogne@163.com; 1059514920@qq.com).

Color versions of one or more figures in this letter are available at https://doi.org/10.1109/LPT.2022.3159964.

Digital Object Identifier 10.1109/LPT.2022.3159964

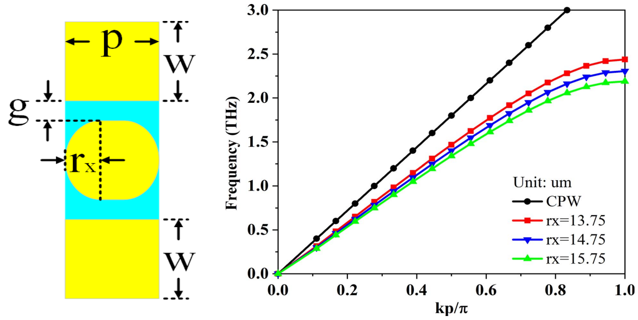

(a) (b)

Fig. 1. (a) The top view of the proposed THz SSPP unit cell. (b) the dispersion curves of CPW and the proposed SSPP unit cell with different parameters.

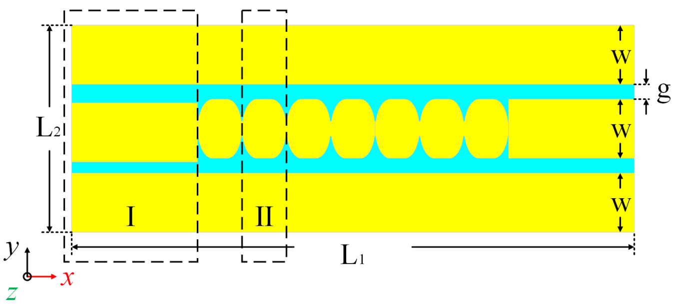

Fig. 2. The top view of the proposed THz SSPP waveguide.

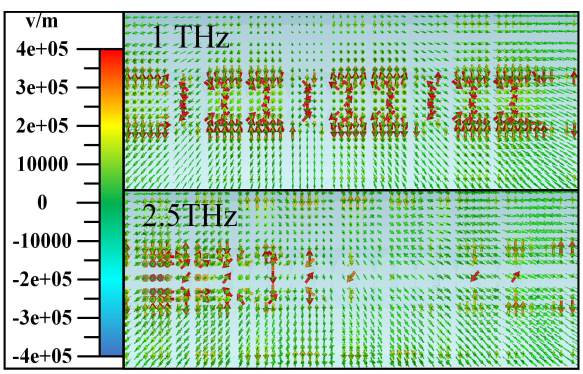

Fig. 3. The electric field distribution of the waveguide on the x-y plane at 1THz and 2.5THz.

the substrate. The blue part represents substrate with a relative dielectric constant of 3.75, a loss tangent of 0.0004, and the thickness is 27.5μm. The yellow part is the metal with 4μm thickness. The width and gap of the CPW line are w and g, respectively. The size of the proposed SSPP unit is denoted by r_x and p. The dispersion curves obtained from numerical eigenmode simulations carried out by the commercial software CST are shown in Fig. 1(b), which indicates that the upper cut-off frequency of the proposed filter can be controlled by changing its geometry dimensions. It is clear that as the parameter r_x increases from 13.75 μm to 15.75 μm, the upper cut-off frequency decreases from 2.34 THz to 2.14 THz.

To more intuitively understand the excellent propagation property of the proposed SSPP-based filter, Fig. 3 shows the simulated electric field distributions on the x-y plane at 1 THz and 2.5 THz. It can be clearly seen that within the cut-off frequency of SSPP waveguide, the structure has good low-pass characteristics.

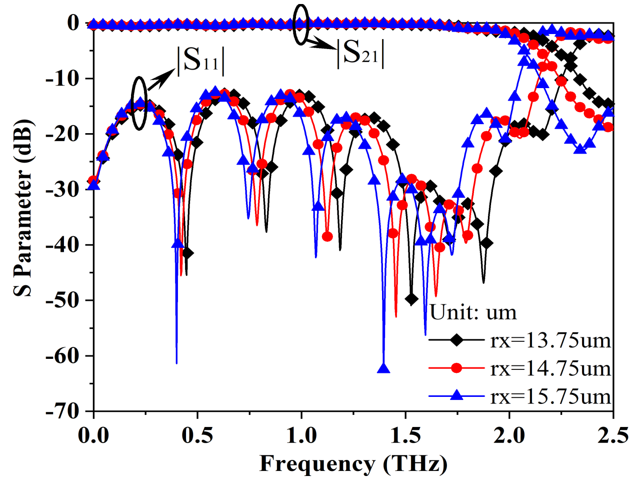

Fig. 4. Simulated S-parameters of the SSPP waveguide with r_x changing from 13.75 μm to 15.75 μm in step of 1 μm.

B. The Proposed SSPP Waveguide and Low-Pass Performance

In order to describe the low-pass performance of SSPP waveguide in detail, the initial parameters of the structure are given as follows: $L_1 = 390.5\mu$m, $L_2 = 146.5\mu$m, t = 4 μm, h = 27.5 μm, $r_x = 14.75\mu$m, W = 19.25 μm, g = 5.5 μm. The transmission and reflection characteristics are shown in Fig. 4, which have high low-pass transmission efficiency. Moreover, it can be seen that the cut-off frequency of the waveguide can be flexibly turned by changing the physical dimensions of SSPP units. As r_x increases from 13.75 μm to 15.75 μm, the upper cut-off frequency reduces from 2.34 THz to 2.14 THz.

C. The Interdigital Structure and the Proposed Band-Pass Filter

In order to realize the low frequency filtering characteristics and control the lower cut-off frequency based on the proposed SSPP waveguide, the interdigital structure is added in the center of the SSPP unit cell, which composes of the proposed band-pass filter design, as shown in Fig. 5(a). Fig. 5(b) gives the structure of SSPP element with interdigital structure.

Fig. 6 shows the transmission and reflection characteristics of the band-pass filter. As l increased from 3.5 μm to 4.5 μm, the lower cut-off frequency decreases from 0.73 THz to 0.59 THz and the upper cut-off frequencies maintain unchanged. It means that the low frequency of the proposed filter can be controlled by changing the geometric parameters of the interdigital structure. Moreover, it can be clearly seen that the proposed filter shows a good band-pass filtering characteristic while maintaining a good out-of-band rejection, the $|S_{21}|$ is lower than -10 dB from 2.18 THz to 2.5 THz when $l = 4$ μm.

TABLE I
COMPARISON TABLE WITH OTHER EXISTING BAND-PASS FILTERS

Ref	Technology	Bandwidth	Relative bandwidth	Size (λ ∗ λ)	Insertion loss of the center frequency (dB)	Controllable frequency
[6]	SIW	0.131 THz - 0.149 THz (3dB)	13.03%	0.56 × 0.37	1.46	No
[8]	Metamaterial	0.297 THz - 0.33 THz (3dB)	10.4%	21 × 23	≈ 2	Yes
[12]	SSPP	0.17 THz - 0.52 THz (3dB)	87.85%	1.7 × 0.13	6	Yes
[24]	SIW+SSPP	0.208 THz -0.256 THz (3dB)	20.7%	0.7 × 0.22	2	Yes
This work	SSPP	0.65 THz - 2.02 THz (2dB)	102.6%	1.56 × 0.6	0.2	Yes

*All of data is the simulated results, λ is the wavelength of the central frequency.

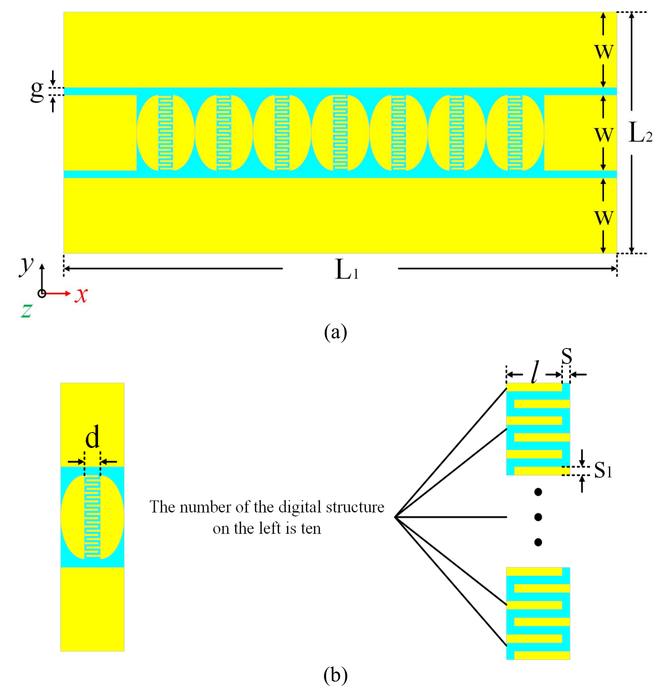

Fig. 5. (a) The top view of the proposed THz SSPP band-pass filter. (b) SSPP element with interdigital structure.

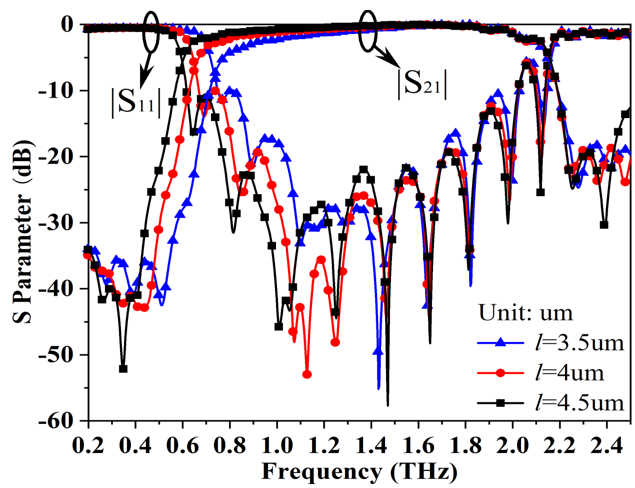

Fig. 6. Simulated S-parameters of the band-pass filter with l changing from 3.5 μm to 4.5 μm in step of 0.5 μm.

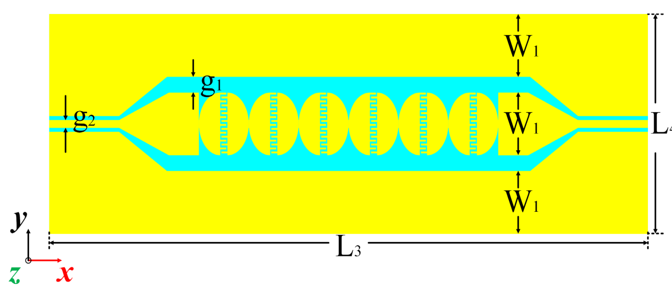

Fig. 7. Diagram of the microwave frequency band-pass filter.

III. EXPERIMENTAL VERIFICATION

A band-pass filter operating at millimeter-wave frequency was fabricated to verify the proposed THz design concept. A special coplanar waveguide conversion part is designed in the filter, which is aimed at convenient detection for probe platform. Fig. 7 shows the proposed millimeter-wave band-pass filter with the conversion part. The thickness of the substrate and metal are 0.127 mm and 0.004 mm, respectively. The dimensions of fabricated millimeter-wave band-pass filter are: $W_1 = 0.64$ mm, $L_3 = 9.38$ mm, $L_4 = 2.024$ mm, $g_1 = 0.052$ mm, $g_2 = 0.14$ mm. Fig. 8(a) and (b) are the fabricated prototype and the testing platform. The simulated and measured results of the proposed design are presented in Fig. 9. The measured insertion loss of the center frequency is 1.1 dB and the return loss is over 10 dB within the passband of 40-100 GHz. The measured results agree well with the simulated ones, which indicates that the design concept for THz band-pass filter has a great potential application in practical engineering in the future.

Table I summarizes the simulated performance comparison of the existing THz filter designs. It can be seen that the filter realized by SIW in [6] achieves a bandwidth from 0.131-0.149 THz, whose relative bandwidth is only 13.03%. The terahertz dual-resonance band-pass filter using bilayer reformative complementary metamaterial structures is proposed in [8], which works at a higher frequency. However, it is limited to its λ relative bandwidth and size. In [12] and [24], two SSPP-based THz filters were proposed, whose bandwidth cover from 0.17-0.52 THz with 87.85% relative bandwidth and 0.208-0.256 THz with 20.7% relative bandwidth.

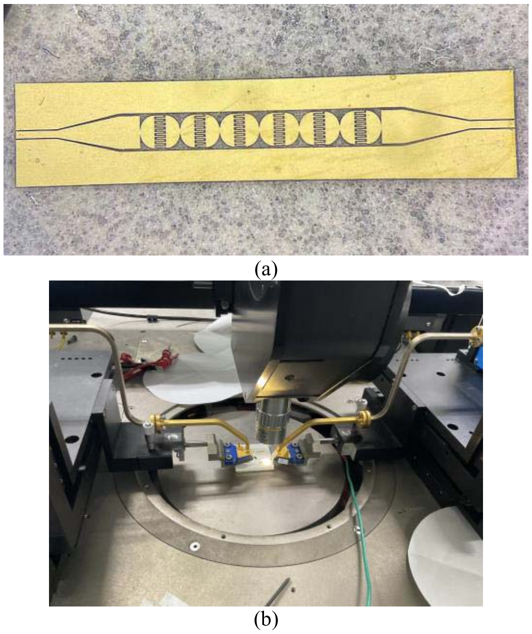

Fig. 8. Photograph of the (a) fabricated band-pass filter (b) test platform.

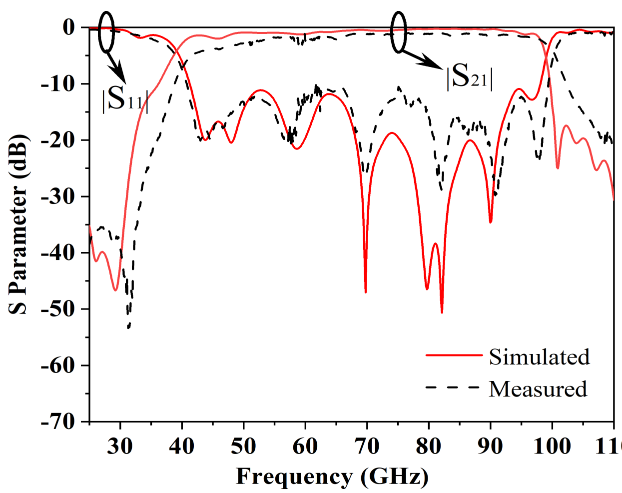

Fig. 9. Measured and simulated S-parameters of the filter.

Compared with other type band-pass filters, the proposed design in this letter exhibits the advantages on bandwidth, relative bandwidth, insertion loss, and controllable frequency.

IV. Conclusion

In this letter, a THz ultra-broadband band-pass filter based on CPW and SSPPs is proposed. The proposed design is analyzed by the dispersion curves and electric field distributions. The lower and upper cut-off frequencies can be tuned by changing the related parameters. A prototype of the band-pass filter operating at millimeter-wave frequency has been fabricated, and the measured results are in good agreement with the simulated ones. The proposed band-pass filter has the advantages of high transmission efficiency, easy frequency adjustment, simple structure and small size, which makes it to be very useful for a wide variety of millimeter-wave and terahertz applications.

References

[1] K. Yang, S. Liu, S. Arezoomandan, A. Nahata, and B. Sensale-Rodriguez, "Graphene-based tunable metamaterial terahertz filters," *Appl. Phys. Lett.*, vol. 105, no. 9, 2014, Art. no. 093105.

[2] Y. Zhu *et al.*, "Terahertz band-pass filters using double-stacked metamaterial layers," *Opt. Lett.*, vol. 37, no. 3, pp. 296–298, Feb. 2012.

[3] Y. Zhu *et al.*, "Tunable dual-band terahertz metamaterial band-pass filters," *Opt. Lett.*, vol. 38, no. 14, pp. 2382–2384, 2013.

[4] X. Zhou, X. Yin, T. Zhang, L. Chen, and X. Li, "Ultrabroad terahertz band-pass filter by hyperbolic metamaterial waveguide," *Opt. Exp.*, vol. 23, no. 9, pp. 11657–11664, 2015.

[5] C. Y. Chen, C. L. Pan, C. F. Hsieh, Y. F. Lin, and R. P. Pan, "Liquid-crystal-based terahertz tunable Lyot filter," *Appl. Phys. Lett.*, vol. 88, no. 10, 2006, Art. no. 101107.

[6] S. W. Wong, K. Wang, Z.-N. Chen, and Q.-X. Chu, "Electric coupling structure of substrate integrated waveguide (SIW) for the application of 140-GHz bandpass filter on LTCC," *IEEE Trans. Compon., Packag., Manuf. Technol.*, vol. 4, no. 2, pp. 316–322, Feb. 2014.

[7] K. Wang, S.-W. Wong, G.-H. Sun, Z. Ning Chen, L. Zhu, and Q.-X. Chu, "Synthesis method for substrate-integrated waveguide bandpass filter with even-order Chebyshev response," *IEEE Trans. Compon., Packag., Manuf. Technol.*, vol. 6, no. 1, pp. 126–135, Jan. 2016.

[8] F. Lan, Z. Yang, L. Qi, X. Gao, and Z. Shi, "Terahertz dual-resonance band-pass filter using bilayer reformative complementary metamaterial structures," *Opt. Lett.*, vol. 39, no. 7, pp. 1709–1712, 2014.

[9] D. Zhang, K. Zhang, Q. Wu, and T. Jiang, "Efficient propagation of spoof surface plasmon polaritons supported by substrate integrated waveguide with bandpass features," *J. Phys. D, Appl. Phys.*, vol. 53, no. 42, Oct. 2020, Art. no. 425104.

[10] Y.-J. Guo, K.-D. Xu, X. Deng, X. Cheng, and Q. Chen, "Millimeter-wave on-chip bandpass filter based on spoof surface plasmon polaritons," *IEEE Electron Device Lett.*, vol. 41, no. 8, pp. 1165–1168, Aug. 2020.

[11] K. D. Xu *et al.*, "Compact millimeter-wave on-chip dual-band bandpass filter in 0.15-μm GaAs technology," *IEEE Electron Device Lett.*, vol. 10, pp. 152–156, 2022.

[12] R. K. Jaiswal, N. Pandit, and N. P. Pathak, "Spoof surface plasmon polaritons based reconfigurable band-pass filter," *IEEE Photon. Technol. Lett.*, vol. 31, no. 3, pp. 218–221, Feb. 1, 2018.

[13] R. K. Jaiswal, N. Pandit, and N. P. Pathak, "Spoof plasmonic-based band-pass filter with high selectivity and wide rejection bandwidth," *IEEE Photon. Technol. Lett.*, vol. 31, no. 15, pp. 1293–1296, Aug. 1, 2019.

[14] D. Zhang *et al.*, "Compact transition enabled broadband propagation of spoof surface plasmon polaritons based on the equivalent circuit model," *J. Phys. D, Appl. Phys.*, vol. 55, no. 16, Apr. 2022, Art. no. 165101.

[15] K.-D. Xu, F. Zhang, Y.-J. Guo, L. Ye, and Y. Liu, "Spoof surface plasmon polaritons based on balanced coplanar stripline waveguides," *IEEE Photon. Technol. Lett.*, vol. 32, no. 1, pp. 55–58, Jan. 1, 2020.

[16] D. Zhang, K. Zhang, Q. Wu, and T. Jiang, "Short-circuited stub-loaded spoof surface plasmon polariton transmission lines with flexibly controllable lower out-of-band rejections," *Opt. Lett.*, vol. 46, no. 17, pp. 4354–4357, Sep. 2021.

[17] L. Pan, Y. Wu, W. Wang, Y. Wei, and Y. Yang, "A flexible high-selectivity single-layer coplanar waveguide bandpass filter using inter-digital spoof surface plasmon polaritons of bow-tie cells," *IEEE Trans. Plasma Sci.*, vol. 48, no. 10, pp. 3582–3588, Oct. 2020.

[18] J. Wang, L. Zhao, and Z.-C. Hao, "A band-pass filter based on the spoof surface plasmon polaritons and CPW-based coupling structure," *IEEE Access*, vol. 7, pp. 35089–35096, 2019.

[19] D. Zhang, K. Zhang, Q. Wu, and T. Jiang, "A compact wideband filter based on spoof surface plasmon polaritons with a wide upper rejection band," *IEEE Photon. Technol. Lett.*, vol. 32, no. 24, pp. 1511–1514, Dec. 15, 2020.

[20] L. Zhao *et al.*, "A novel broadband band-pass filter based on spoof surface plasmon polaritons," *Sci. Rep.*, vol. 6, no. 1, p. 36069, Oct. 2016.

[21] L. Ye *et al.*, "Super subwavelength guiding and rejecting of terahertz spoof SPPs enabled by planar plasmonic waveguides and notch filters based on spiral-shaped units," *J. Lightw. Technol.*, vol. 36, no. 20, pp. 4988–4994, Oct. 15, 2018.

[22] J. Wang, L. Zhao, Z.-C. Hao, and T. J. Cui, "An ultra-thin coplanar waveguide filter based on the spoof surface plasmon polaritons," *Appl. Phys. Lett.*, vol. 113, no. 7, Aug. 2018, Art. no. 071101.

[23] Y. Cui, K.-D. Xu, Y.-J. Guo, and Q. Chen, "Half-mode substrate integrated plasmonic waveguide for filter and diplexer designs," *J. Phys. D, Appl. Phys.*, vol. 55, no. 12, Mar. 2022, Art. no. 125104.

[24] H. Zhu, Y. Zhang, L. Ye, Y. Li, Y. Xu, and R. Xu, "On-chip terahertz bandpass filter based on substrate integrated plasmonic waveguide," *Results Phys.*, vol. 27, Aug. 2021, Art. no. 104553.